



Original articles

Research article

<https://doi.org/10.17308/kcmf.2022.24/9265>

Growth of InGaAsSb/GaSb compound for infrared optoelectronic devices

Tien Dai Nguyen^{1,2✉}, J. O. Kim³, S. J. Lee^{3✉}¹*Institute of Theoretical and Applied Research,
Duy Tan University, Hanoi 100000, Vietnam*²*Faculty of Natural Sciences, Duy Tan University,
Da Nang 550000, Vietnam*³*Metrology of Future Technology, Korea Research Institute of Standards and Science,
Daejeon 34113, South Korea*

Abstract

In this study, we report on the synthesis of InGaAsSb epi-layer for optoelectronic devices in short infrared wavelengths (SWIR) at room temperature (RT).

The InGaAsSb with lattice matched to GaSb substrate was grown by the molecular beam epitaxy (MBE) using the strain engineering. The structural and optical properties of InGaAsSb layer was investigated by high resolution X-ray diffractometer (XRD), and photoluminescence (PL). Devices with a 400×400 μm of size were fabricated using traditional photolithography and inductively coupled plasma etching. The spectral response of InGaAsSb photodetector with a 90% cutoff wavelength and electroluminescence spectra of light emitting diode (LED) obtained at 2.38 μm at an applied bias of –0.1 V and 2.25 μm with $J_{ic} = 500$ mA, respectively at room temperature. Also, the spectral response of the detector indicates an increasing intensity and low noise when the temperature is high.

Keywords: InGaAsSb; MBE, Optoelectronic device, SWIR**Funding:** This work was supported by the Korea Evaluation Institute of Industrial Technology (KEIT) grant 10052824 funded by the Korea government (MOTIE) and the Institute of Theoretical and Applied Research (ITAR), Duy Tan University.**For citation:** Nguyen T. D., Kim J. O., Lee S. J. Growth of InGaAsSb/GaSb compound for infrared optoelectronic devices. *Condensed Matter and Interphases*. 2022;24(2): 250–255. <https://doi.org/10.17308/kcmf.2022.24/9265>**Для цитирования:** Нгуен Т. Д., Ким Д. О., Ли С. Д. Выращивание соединения InGaAsSb/GaSb для инфракрасных оптоэлектронных приборов. *Конденсированные среды и межфазные границы*. 2022;24(2): 250–255. <https://doi.org/10.17308/kcmf.2022.24/9265>✉ Nguyen Tien Dai, e-mail: nguyentien dai@duytan.edu.vn✉ Lee S. J., e-mail: sjlee@kriss.re.kr

© Nguyen T. D., Kim J. O., Lee S. J., 2022



1. Introduction

Infrared (IR) light-emitting diode (LED) and short wavelength IR detector (SWIR, 1.7–3 μm) are useful for various infrared applications (academia, industry, military, especially, atmospheric remote sensing, and gas detection) [1–7]. The antimony (Sb) material based III–V semiconductor compound is a promising candidate for the development of IR-detectors and -LED devices in short and mid wavelength IR range. Especially, the quaternary InGaAsSb compound has been interesting for the IR optoelectronic devices [8, 9]. The InGaAsSb based LED and photodetectors might be used for optical sensing (CO, CO₂, and CH₄ gas detections) due to lower noise, high sensitive, and high output power issues [3, 10]. The InGaAsSb compounds have been grown by many epitaxial systems such as metalorganic vapour phase epitaxy (MOVPE), [11] liquid phase epitaxy (LPE) [12] and molecular beam epitaxy (MBE) [13]. Among them, the MBE has several advantages such as lower growth temperature and precise control of the epi-thickness and composition. Therefore, in this study, we report on growth InGaAsSb/GaSb compound for IR detector and LED devices using MBE growth approach. The crystalline, morphological and optical properties of epi-layers (InGaAsSb and Al(Ga)AsSb) were investigated. Based on this result, we fabricated the full structure of photodetector and LED. Characterizations (spectral response, current–voltage and spectral

electroluminescence) of InGaAsSb devices are studied at room temperature.

2. Experimental

2.1. Growth of infrared photodetector

Fig. 1(a) shows the schematic of InGaAsSb photodetector with the *n* type-barrier-*n* type layer (*nBn*) structure design. This InGaAsSb composition layer was proposed to control lattice-matched on the *n*⁺-GaSb (100) substrate. Layers were grown by the molecular beam epitaxy (MBE) system (RIBER 32P) using As₂ and Sb₂ cracker sources. The stack of layers consisted of a bottom contact, *n*⁺-In_{*x*}Ga_{*1-x*}As_{*y*}Sb_{*1-y*} ($2 \cdot 10^{18} \text{ cm}^{-3}$) with thickness of 300 nm, a 300 nm thick *n*⁺-GaSb ($2 \cdot 10^{18} \text{ cm}^{-3}$) buffer, and a top contact of *n*⁺-GaSb ($2 \cdot 10^{18} \text{ cm}^{-3}$), which was 200 nm thick. A 2 μm thick *n*-In_{*x*}Ga_{*1-x*}As_{*y*}Sb_{*1-y*} ($2 \cdot 10^{16} \text{ cm}^{-3}$) active sandwich structure (*nBn*) between the top and bottom contacts consisted of InGaAsSb where the composition of indium was 17%, while composition of As was 15%, a 2 μm thick *n*-In_{*x*}Ga_{*1-x*}As_{*y*}Sb_{*1-y*} ($2 \cdot 10^{16} \text{ cm}^{-3}$). An unipolar barrier of Al_{*0.5*}Ga_{*0.7*}Sb with 60 nm thick was grown on the active layer. The InGaAsSb layer was characterized by high resolution X-ray diffractometer (XRD). The XRD results indicated that the InGaAsSb layer was lattice matched to the GaSb substrate, as shown in Fig. 2(a) [14].

2.2. Growth of infrared light emitting diode

Fig. 1. (b) shows a detailed schematic of LED structure, which consists of three

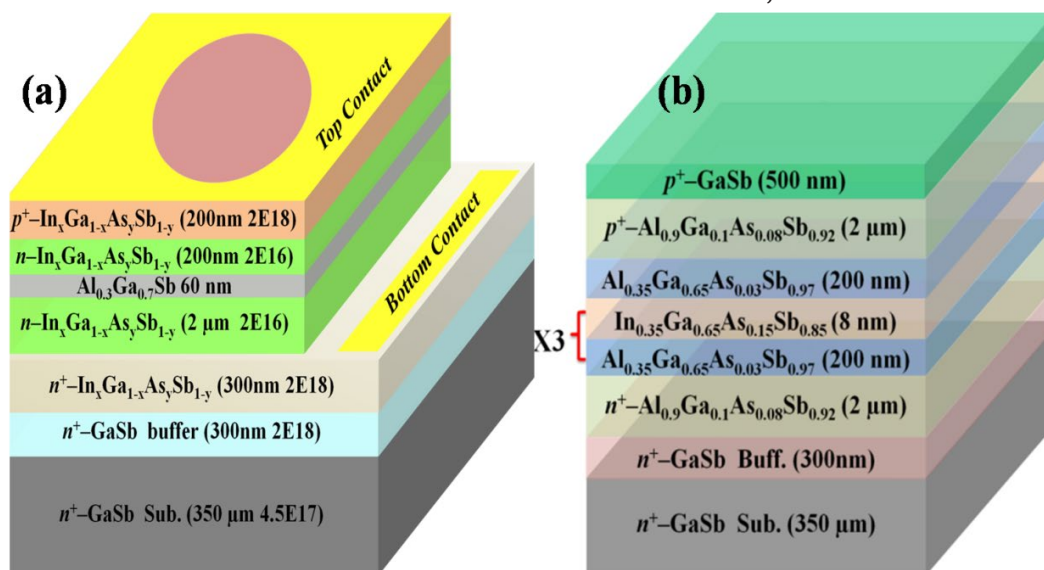


Fig. 1. (Color online) (a) Layer structure of IR-photodetector (b) Layer structure of IR-LED

$\text{In}_{0.35}\text{Ga}_{0.65}\text{As}_{0.15}\text{Sb}_{0.85}/\text{Al}_{0.35}\text{Ga}_{0.65}\text{As}_{0.05}\text{Sb}_{0.97}$ quantum wells with an 8 nm/200 nm thick, respectively. Following the $\text{In}_{0.35}\text{Ga}_{0.65}\text{As}_{0.15}\text{Sb}_{0.85}$ active layer is a 2 μm thick $n(p)\text{-Al}_{0.9}\text{Ga}_{0.1}\text{As}_{0.08}\text{Sb}_{0.92}$ ($1\cdot 10^{18}\text{ cm}^{-3}$) cladding and capping layers. A 500 nm thick $p^+\text{-GaSb}$ ($1\cdot 10^{18}\text{ cm}^{-3}$) was grown for top contact. The substrate temperature for growth InGaAsSb layer was at temperature of 460 °C, while that of the other layers (AlGaAsSb cladding, and barrier) was grown at temperature of 480 °C [14, 15].

2.3. Device fabrication

The photodetector device with a mesa size of $400\times 400\ \mu\text{m}$ was processed using photolithography and inductively coupled plasma etching. The ohmic contact metals with Ge/Au/Ni/Au layers were deposited by the electron beam evaporation (EBV) on the contact layer. The contacts were annealed at temperature of 200 °C using rapid thermal annealing. The detector had a circular aperture of 300 μm in each mesa, as shown in Fig. 3(a). The device was mounted on a leadless chip carrier for characteristics. Besides, the contact metals of Ti/Pt/Au were also deposited by the EBV on the $p\text{-GaSb}$ contact for LED device. The GaSb substrate was lapped and polished down to about 200 μm thick with a roughness of 12 nm. The LED die with a $400\times 400\ \mu\text{m}$ size was fabricated using photolithography, as shown in Fig. 3 (b). The top contact metals of Ge/Au/Ni/Au were deposited. After the device process, the

sample was mounted and wire-bonded onto a standard TO-18 package and a leadless chip carrier, as shown in Fig. 3 (c) [14].

3. Results and discussion

3.1. Characterizations of IR detector

In Fig. 4(a), the dark current density of detector measured at different temperatures using a Keithley 236. At the temperature range of 200–300 K, voltage–current curves exhibit an asymmetric shape that is attributed to the effect of a unipolar barrier ($\text{Al}_{0.5}\text{Ga}_{0.7}\text{Sb}$) [6]. Fig. 4 (b) shows the spectral response of a detector, which was measured by the Fourier transform infrared (FTIR-Nicolet 5700), using a white source and KBr window. The device exhibited the redshift of spectral when we carried out the increasing temperature from 100–300 K with a 90% cutoff wavelength from 1.95 to 2.38 μm . The cutoff wavelength of the device matches our calculation of $\text{In}_{0.17}\text{Ga}_{0.83}\text{As}_{0.15}\text{Sb}_{0.85}$ compound at 300 K. In order to match this cutoff wavelength, the composition of an InGaAsSb could be controlled due to both In and As concentrations [16, 17]. Also, the spectral response of the detector indicates an increasing intensity and low noise when the temperature is high. This phenomenon is attributed to the carrier blocking the effect of the AlGaSb barrier layer and re-align the band offset of the valance region. Thus, this mechanism

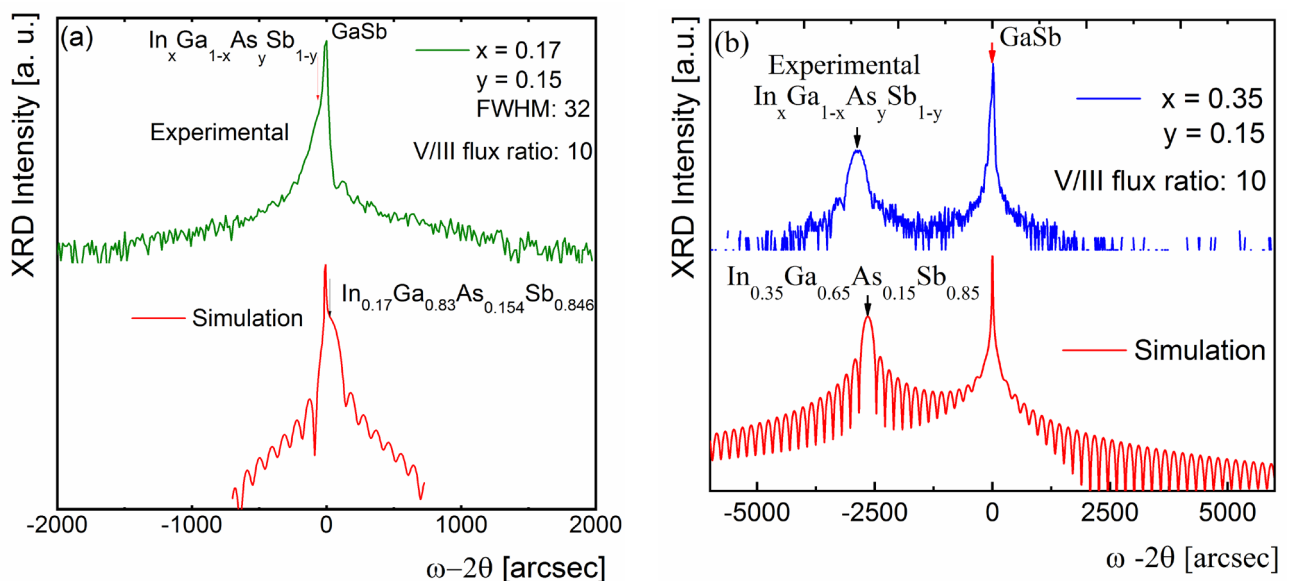


Fig. 2. (Color online) (a) X-ray diffraction rocking curve (004) planes of an $\text{In}_{0.17}\text{Ga}_{0.83}\text{As}_{0.15}\text{Sb}_{0.85}$ alloy for detector (b) optimization of $\text{In}_{0.35}\text{Ga}_{0.65}\text{As}_{0.15}\text{Sb}_{0.85}$ alloy for LED

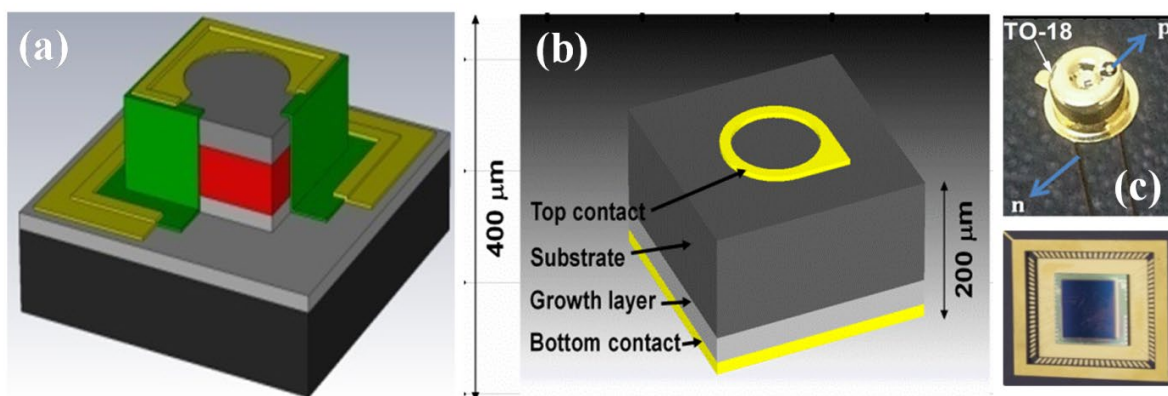


Fig. 3. (Color online) (a) Schematic view of single photodiode, (b) light emitting diode device and (c) mounted in standard TO–18 package and leadless chip carrier

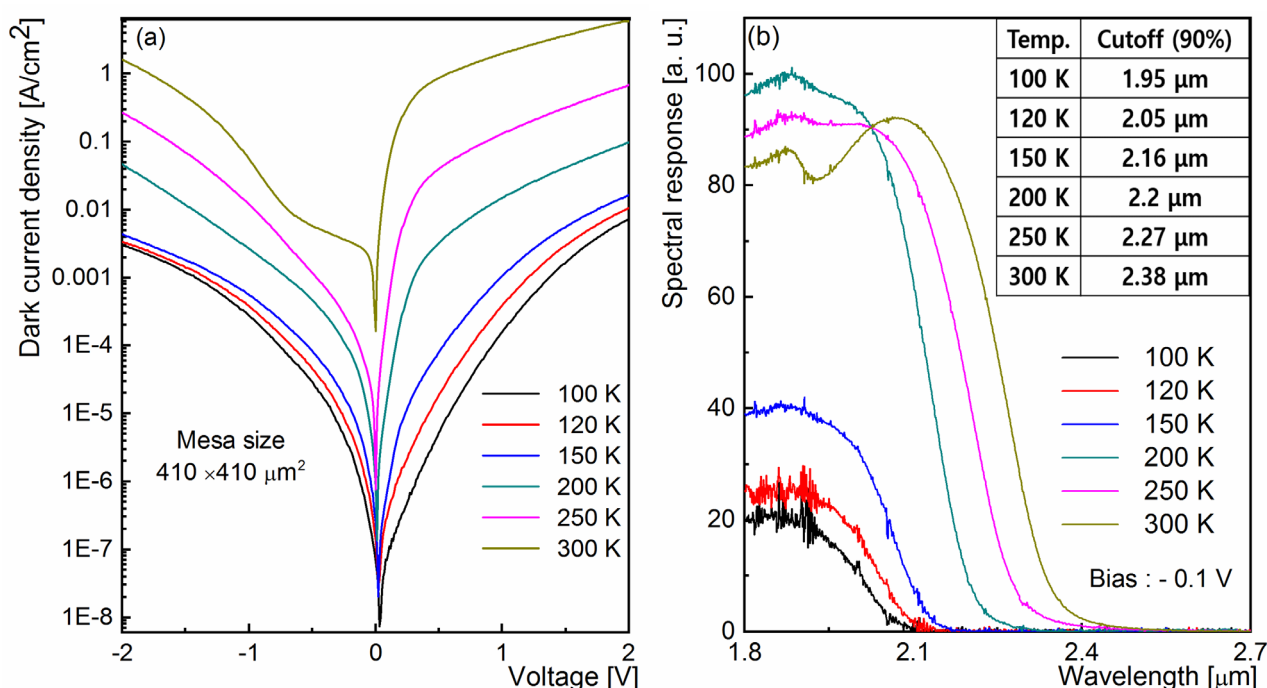


Fig. 4 (Color online) (a) The temperature depends on the dark current density of photodetector (b) Spectral response of the 90% cutoff wavelength shifts from 1.95 to 2.38 μm at temperature of 100–300 K

needs to detail the study by simulation approach.

3.2. Characterizations of light emitting diode

Fig. 5(a) is a current–voltage (I - V) of the LED at room temperature that shows a clear rectifying behavior with a turn–on voltage of about 0.35 V and an exponential increase in the forward current with increasing forward bias voltage. Due to this turn on voltage, we only supply a small potential that the photon easily emits from the active layer under suitable injection current (J_{ic}) condition. The series resistance, R_s , is 12.3 Ω, which was evaluated from the slope of I - V curve of LED device at room temperature. The small R_s value implies a well ohmic contact between GaSb

and metal layers. However, this value is still high compared to a commercial LED device (~3–5 Ω) that is the effect of the injection current on out power efficiency of the LED device.

In Fig. 5(b), the electroluminescence (EL) characteristic of IR–LED shows at room temperature. The peak of spectral EL is at 2.25 μm with 161 nm of full width haft maximum (FWHM) under injection current of 500 mA. The spectral EL is a recombination of electron–hole pairs of the first quantized level when the transmit from the conduction band to the valence band of a quantum well, as seen inserted picture in Fig. 5(b). There are two shoulder peaks at 1.96 μm

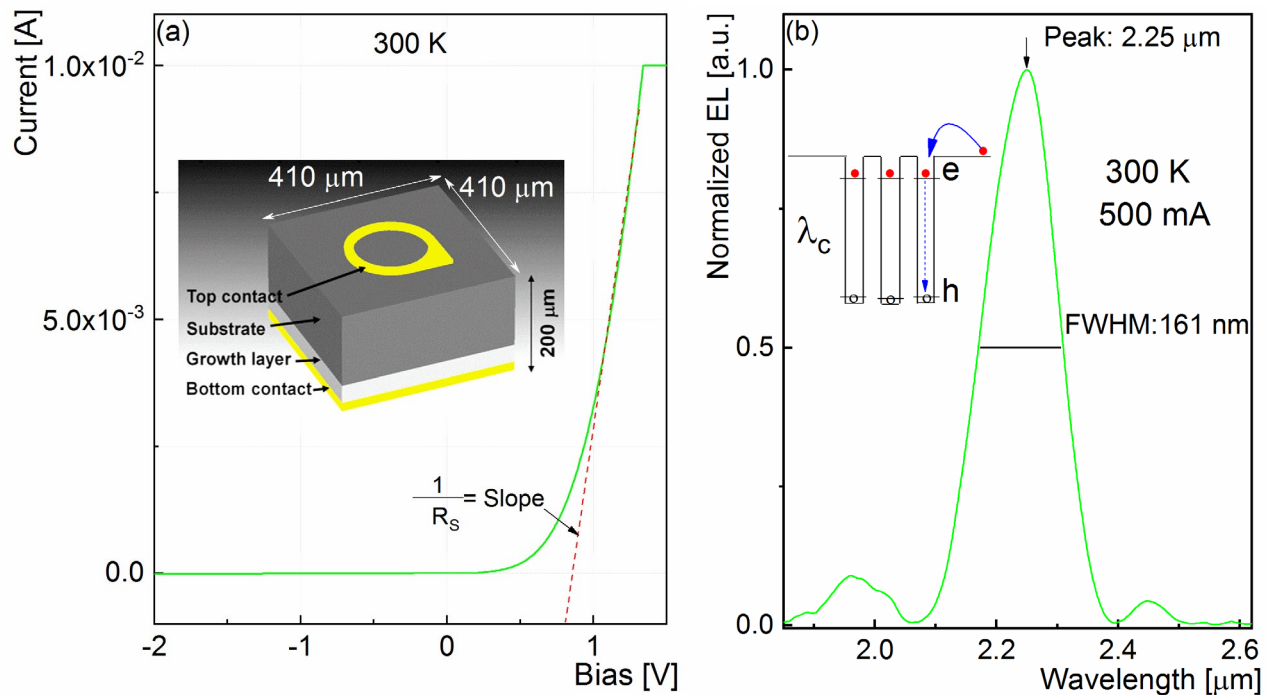


Fig. 5. (Color online) (a) Current–voltage, (b) Spectral electroluminescence characterizations of the IR light emitting diode measured at temperature of 300 K

and 2.45 μm , which is attributed to the effect of a thermal generation when LED die undergone a high injection current ($J_{ic} = 500 \text{ mA}$). As mention in above paragraph, the injection current is higher than the commercial LED (50 mA) due to the larger series resistance. This parameter should be optimized by the treatment of GaSb surface, optimized RTA condition, and change the metal contacts for improving output power efficiency.

4. Conclusions

We grew InGaAsSb epi-layer lattice matched to GaSb for infrared photodetector and light emitting diode, LED. By using the MBE approach, structural devices (nBn for photodetector and quantum well for LED) were synthesized. The photodetector obtained the spectral response at 2.38 μm , under the applied bias of -0.1 V, while LED shows spectral emission peak of 2.25 μm (FWHM = 161 nm) with injection current of 500 mA at room temperature. Based on those results, those optoelectronic devices might be served for spectrometers and with nondispersive infrared, NDIR, sensor.

Acknowledgements

This work was supported by the Korea Evaluation Institute of Industrial Technology

(KEIT) grant 10052824 funded by the Korea government (MOTIE) and the Institute of Theoretical and Applied Research (ITAR), Duy Tan University.

Conflict of interest

The authors declare that they have no known competing financial interests or personal relationships that could have influenced the work reported in this paper

References

1. Benoit J., Boulou M., Soulage G., Joullie A., Mani H. Performance evaluation of GaAlAsSb/GaInAsSb SAM-APDs for high bit rate transmissions in the 2.5 μm wavelength region. *Journal of Optical Communications*. 1988;9(2): 55. <https://doi.org/10.1515/joc.1988.9.2.55>
2. Carter B. L., Shaw E., Olesberg J. T., Chan W. K., Hasenberg T. C., Flatte M. E. High detectivity GaInAsSb pin infrared photodetector for blood glucose sensing. *Electronics Letters*. 2000;36(15): 1301–1303. <https://doi.org/10.1049/el:20000956>
3. Suchalkin S., Jung S., Kipshidze G., Shterengas L., Hosoda T., Westerfeld D., Snyder D., Belenky G. GaSb based light emitting diodes with strained InGaAsSb type I quantum well active regions. *Applied Physics Letters*. 2008;93(8): 081107. <https://doi.org/10.1063/1.2974795>

4. Gibson D., MacGregor C. A novel solid state non-dispersive infrared CO₂ gas sensor compatible with wireless and portable deployment. *Sensors*. 2013;13(6): 7079–7103. <https://doi.org/10.3390/s130607079>
5. Craig A. P., Jain M., Wicks G., Golding T., Hos-sain K., McEwan K., Howle C., Percy B., Marshall A. R. J. Short-wave infrared barricide detectors using InGaAsSb absorption material lattice matched to GaSb. *Applied Physics Letters*. 2015;106(20): 201103. <https://doi.org/10.1063/1.4921468>
6. Martyniuk P., Kopytko M., Rogalski A. Barrier infrared detectors. *Opto-Electronics Review*. 2014;22(2): 127–146. <https://doi.org/10.2478/s11772-014-0187-x>
7. Hoang A. M., Dehzangi A., Adhikary S., Razeghi M. High performance bias-selectable three-color short-wave/mid-wave/long-wave infrared photodetectors based on type-II InAs/GaSb/AlSb superlattices. *Scientific Reports*. 2016;6(1): 24144. <https://doi.org/10.1038/srep24144>
8. Scholz L., Perez A. O., Knobelspies S., Wöllenstein J., Palzer S. MID-IR LED-based, photoacoustic CO₂ sensor. *Procedia Engineering*. 2015;120: 1233–1236. <https://doi.org/10.1016/j.proeng.2015.08.837>
9. Refaat T. F., Abedin M. N., Koch G. J., Singh U. N. InGaAsSb detectors' characterization for CO₂ Lidar/DIAL applications. *NASA Langley Research Center; Hampton, VA, 23681-2199*. United States: 2003. p. 32.
10. Joullié A., Christol P. GaSb-based mid-infrared 2–5 μm laser diodes. *Comptes Rendus Physique*. 2003;4(6): 621–637. [https://doi.org/10.1016/s1631-0705\(03\)00098-7](https://doi.org/10.1016/s1631-0705(03)00098-7)
11. Cherng M. J., Jen H. R., Larsen C. A., Strigfellow G. B., Lundt H., Taylor P. C. MOVPE growth of GaInAsSb. *Journal of Crystal Growth*. 1986;77(1-3): 408–417. [https://doi.org/10.1016/0022-0248\(86\)90331-3](https://doi.org/10.1016/0022-0248(86)90331-3)
12. Gong X., Yang B., Ma Y., Gao F., Yu Y., Han W., Lui X., Xi J., Wang Z., Lin L. Liquid phase epitaxy growth and properties of GaInAsSb/AlGaAsSb/GaSb heterostructures. *Japanese Journal of Applied Physics*. 1991;30(7R): 1343–1347. <https://doi.org/10.1143/jjap.30.1343>
13. Reddy M. H. M., Olesberg J. T., Cao C., Pri-neas J. P. MBE-grown high-efficiency GaInAsSb mid-infrared detectors operating under back illumination. *Semiconductor Science and Technology*. 2006;21(3): 267–272. <https://doi.org/10.1088/0268-1242/21/3/009>
14. Kim J. O., Nguyen T. D., Ku Z., Urbas A., Kang S.-W., Lee S. J. Short wavelength infrared photodetector and light emitting diode based on InGaAsSb. *Infrared Technology and Applications XLIII*. 2017. <https://doi.org/10.1117/12.2264969>
15. Nguyen T. D., Hwang J., Kim Y., Kim E.-T., Kim J. O., Lee S. J. Dual-wavelength InGaAsSb/AlGaAsSb quantum-well light-emitting diodes. *Journal of the Korean Physical Society*. 2018;72(10): 1249–1253. <https://doi.org/10.3938/jkps.72.1249>
16. Nguyen T. D., Kim J. O., Kim Y. H., Kim E. T., Nguyen Q. L., Lee S. J. Dual-color short-wavelength infrared photodetector based on InGaAsSb/GaSb heterostructure. *AIP Advances*. 2018;8(2): 025015. <https://doi.org/10.1063/1.5020532>
17. Reddy M. H. M., Olesberg J. T., Cao C., Pri-neas J. P. MBE-grown high-efficiency GaInAsSb mid-infrared detectors operating under back illumination. *Semiconductor Science and Technology*. 2006;21(3): 267–272. <https://doi.org/10.1088/0268-1242/21/3/009>

Information about the authors

Tien Dai Nguyen, PhD in Advanced Materials Science and Engineering, Lecturer/ Research at Institute of Theoretical and Applied Research (ITAR), Duy Tan University (DTU) (Hanoi, Vietnam).

<https://orcid.org/0000-0002-9420-210X>
nguyentien dai@duytan.edu.vn

J. O. Kim, PhD in Physics; Senior Researcher, Advanced Instrumentation Institute, Korea Research Institute of Standards and Science (Yuseong-gu, Daejeon, South Korea).
jokim@kriss.re.kr

S. J. Lee, PhD in Physics, Principal Research Scientist, Korea Research Institute Standards and Science (KRISS) Associate Professor at University of Science and Technology (UST) (Yuseong-gu, Daejeon, South Korea).

sjlee@kriss.re.kr

Received 24.01.2022; approved after reviewing 04.03.2022; accepted 15.03.2022; published online 25.06.2022.